

# One to Multiple Mapping Dual Learning: Learning Multiple Sources from One Mixed Signal

Ting Liu, Wenwu Wang, Xiaofei Zhang, Zhenyin Gong, and Yina Guo

**Abstract**—Single channel blind source separation (SCBSS) refers to separate multiple sources from a mixed signal collected by a single sensor. The existing methods for SCBSS mainly focus on separating two sources and have weak generalization performance. To address these problems, an algorithm is proposed in this paper to separate multiple sources from a mixture by designing a parallel dual generative adversarial Network (PDualGAN) that can build the relationship between a mixture and the corresponding multiple sources to realize one-to-multiple cross-domain mapping. This algorithm can be applied to any mixed model such as linear instantaneous mixed model and convolutional mixed model. Besides, one-to-multiple datasets are created which including the mixtures and corresponding sources for this study. The experiment was carried out on four different datasets and tested with signals mixed in different proportions. Experimental results show that the proposed algorithm can achieve high performance in peak signal-to-noise ratio (PSNR) and correlation, which outperforms state-of-the-art algorithms.

**Index Terms**—Single channel blind source separation, parallel dual generative adversarial network, one-to-multiple mapping, dual learning.

## I. INTRODUCTION

The problem of separating sources from a mixed signal collected by a sensor, known as single channel blind source separation (SCBSS), is of paramount importance and difficulty, is widely applied in speech, image and EEG signal processing [1] [2] [3], biomedical engineering [4] [5] [6], multi-source phase retrieval [7] [8] [9], and Eddy current pulsed thermography [10].

Many approaches have been proposed to address the problem of SCBSS, which are mainly divided into two types: approaches for linear instantaneous mixed model and approaches for convolutional mixed model [11]. The former approaches mainly including design the optimal filter (such as Wiener filter) [12] [13], Virtual multi-channel methods (such as empirical mode decomposition (EMD), independent component analysis (ICA) based ensemble empirical mode decomposition (EEMD), non-negative matrix factorization (NMF)) [14] [15] [16] [17] [18] [19], and multi-source phase retrieval [7] [8] [9]. The latter approaches mainly including deep learning approaches based on generative adversarial networks (GANs) (such as GAN-NMF [20], synthesis-decomposition (S-D)

[21]), and single channel blind deconvolution algorithm based on deep convolution generating adversarial network (DCSS) [22]. These approaches are the focus of this paper.

The methods for linear instantaneous mixed model have relatively low algorithm complexity, but they are not suitable for separating non-stationary random signals without prior knowledge and not easy to separate multi-source signals, and NMF may ignore the phase. The methods for convolutional mixed model can separate two sources well, but are not easy to separate multiple signals and have weak generalization. Obviously, these approaches can separate two signals well, but they are not suitable for separating multi-source signals and have weak generalization performance, besides, they are only focused on linear instantaneous mixed model or approaches for convolutional mixed model, but not together.

In real life, due to the limitation of conditions and other factors, such as, the collected electroencephalogram (EEG) signals are often mixed with interference signals of electrocardiogram (ECG), electromyography (EMG), and eye movement artifacts (EOG); the recorded remote sensing images are often obscured by clouds and fog; due to the erosion of time, the loss of ancient Chinese characters often occurs in unearthed cultural relics and ancient books; fingerprint images obtained from criminal investigation scenes often have multiple fingerprints overlapping each other; in a noisy environment, multiple speakers are talking simultaneously, which rise the challenge of its enhanced responsibilities that multiple sources need to be separated from a mixed signal. To our knowledge, there is no existing effective method to address the multi-source separating problem and improve the generalization performance.

The aim of this paper is to address the problem of single channel blind source separation of multiple signals that are applied to both linear instantaneous mixed model and convolutional mixed model and improve the generalization performance. The virtual multi-channel methods are conventional methods that can be thought of, but these methods, such as EMD, separate multiple signals from one mixed signal based on characteristics, and assume that the signals are independent of each other, and the effect is not satisfactory. Recently, generative adversarial Network GAN has received widely attention by researchers, the dual learning and GAN [23] can build one-to-one mapping to realize image-to-image translation. Inspired by this, we design a parallel dual generative adversarial Network (PDualGAN) to realize one-to-multiple mapping, and transform the problem of SCBSS into a data conversion problem in different domains, multiple sources can be separated from a mixture by building the mapping relation

Ting Liu, Xiaofei Zhang, Zhenyin Gong, and Yina Guo are with the Department of Electronics and Communication Engineering, Taiyuan University of Science and Technology, Taiyuan, 030024, China. Corresponding author's e-mail: zulibest@163.com.

Wenwu Wang is with the Centre for Vision, Speech and Signal Processing, University of Surrey, Guildford, Surrey GU2 7XH, U.K. Ting Liu and Wenwu Wang contributed equally to this work. (e-mail: liuting328511@163.com, w.wang@surrey.ac.uk)

between a mixture and multiple corresponding sources. Our contributions are as follows:

- 1) Model. According to the traditional linear instantaneous mixed model and convolutional mixed model, we have discovered the common rules and found the relevant expressions to describe the two models for our research.
- 2) PDualGAN algorithm. Based on the linear instantaneous mixed model and convolutional mixed model, inspired by DualGAN, an algorithm is proposed by introducing parallel dual generative adversarial Network (PDualGAN), one-to-multiple training is performed on the mixtures and corresponding multiple sources, the stability of the network and the quality of the generated data are improved by applying the WGAN-GP loss function, thereby potentially enhancing the performance of multiple sources separation.
- 3) Datasets. One-to-multiple datasets are created for this study which is composed of two parts: the mixtures and corresponding original sources. Each mixture is mixed in a random proportion by multiple corresponding sources which are randomly selected. The datasets can be applied to research related to blind source separation and signal processing, such as speech signal processing, image deconvolution and phase retrieval and blind separation of EEG signals, etc.

This paper is organized as follows: Section II describes the background. Section III builds a one-to-multiple model for the SCBSS problem. Section IV presents our PDualGAN algorithm for the problem of SCBSS. Section V shows the experimental results. Section VI concludes the paper and draws future research directions.

## II. BACKGROUND

As we all know, training on much smaller training datasets while maintaining nearly the same accuracy would be very beneficial. 'less than one' - shot learning [24] can learn  $N$  new classes given only  $M < N$  examples with the help of distance-weighted soft-label prototype k-Nearest Neighbors (SLaPkNN).

**Definition 1:** A hard label is a vector of length  $N$ , indicating that the membership of a point is exactly one of the  $N$  classes.

**Definition 2:** A soft label is a vector representation of a points simultaneous membership to multiple classes.

**Definition 3:** soft label prototype (SLaP) is a pair of vectors  $(X, Y)$ , where  $X$  is a feature (or position) vector, and  $Y$  is an associated soft label.

k nearest neighbor (kNN) [25] only uses hard labels. When a space is partitioned using the classic kNN classifier rule, it is clear that at least  $n$  points are required to separate  $n$  classes. SLaPkNN is a combination of SLaP and kNN, and it generalizes the soft label prototype of kNN, which can be applied to separate  $N$  classes effectively by using only  $M < N$  soft label prototypes. such as a SLaPkNN classifier is fitted

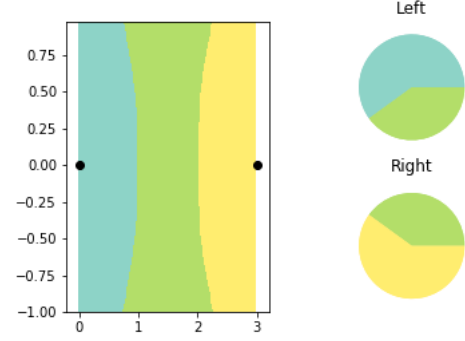


Fig. 1. The soft label distribution of each prototype is illustrated by the pie charts.

on two soft-label prototypes and partitions the space into three classes, as shown in Fig. 1.

Although the 'less than one' - shot learning requires labels in training and is not suitable for processing mixed signals, we are inspired by this and think of an unsupervised mapping method to establish the relationship between the unlabeled and unpaired data.

A generative adversarial network (GAN) is a deep learning model and one of the most promising methods for unsupervised learning in recent years. The model produces good output through adversarial learning of the generator and the discriminator [26]. However, the original GAN algorithm is not suitable for one-to-one conversion tasks between paired data.

Inspired by GAN and dual learning [27] from natural language translation, a dual generative adversarial Network (DualGAN) [23] is developed for one-to-one unlabeled data from two domains. The original GAN has the limitation that it can only learn to translate data from domain  $U$  to those in domain  $V$ , but the DualGAN can learn to invert the task.

Given two sets of unpaired and unlabeled data selected from domains  $U$  and  $V$ , firstly, the task of the DualGAN [23] is to learn a generator  $G_A: U \rightarrow V$ , a mapping relation is built from  $u \in U$  to  $v \in V$ , secondly, the dual task is to train an inverse generator  $G_B: V \rightarrow U$ , and a mapping relation is built from  $v \in V$  to  $u \in U$ . This is realized with two GANs which have the same structure. The original GAN learns the generator  $G_A$  and discriminator  $D_A$  that discriminates between the fake and real data of domain  $V$ . Similarly, the dual GAN learns the generator  $G_B$  and a discriminator  $D_B$ . The overall working process is shown in Fig. 2.

The  $u \in U$  is translated to Domain  $V$  with  $G_A$ . The fitting degree of  $G_A(u, z)$  ( $z$  is a random noise) is evaluated by  $D_A$ . Then,  $G_A(u, z)$  is translated back to domain  $U$  with  $G_B$ , and output  $G_B(G_A(u, z), z')$  ( $z'$  is also a random noise) as a reconstruction of  $u$ . Similarly,  $v \in V$  is translated to Domain  $U$  as  $G_B(v, z')$  with  $G_B$ , and then reconstructed as  $G_A(G_B(v, z'), z)$  with  $G_A$ . The discriminator  $D_A$  is trained with  $v$  as true data and  $G_A(u, z)$  as fake data, however,  $D_B$  takes  $u$  as true and  $G_B(v, z')$  as fake. The generators  $G_A$  and  $G_B$  are trained and optimized to output fake samples to cheat the corresponding discriminators  $D_A$  and  $D_B$ , and to minimize the reconstruction error  $\|v - G_A(G_B(v, z'), z)\|$  and  $\|u - G_B(G_A(u, z), z')\|$ .

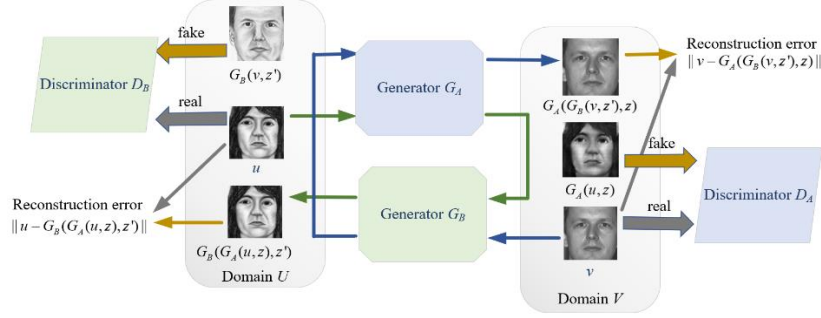


Fig. 2. Working process of DualGAN.

The cross-entropy loss function of the original GAN [26] is substituted by the loss function of Wasserstein GAN (WGAN) [28], which performs better in generator convergence and data quality, and in improving the stability of the network. The loss function applied in  $D_A$  and  $D_B$  can be written as

$$I_A^d(u; v) = D_A(G_A(u; z)) - D_A(v); \quad (1)$$

$$I_B^d(u; v) = D_B(G_B(v; z')) - D_B(u); \quad (2)$$

where  $u \in U$  and  $v \in V$ .

The same loss function is applied in generators  $G_A$  and  $G_B$  as they have the same objective which adopts  $L_1$  distance to measure the reconstruction losses, it can be written as

$$\begin{aligned} I^g(u; v) = & \lambda_U \|u - G_B(G_A(u; z); z')\| \\ & + \lambda_V \|v - G_A(G_B(v; z'); z)\| \\ & - D_B(G_B(v; z')) - D_A(G_A(u; z)) \end{aligned} \quad (3)$$

where  $\lambda_U, \lambda_V$  are both constant parameters which are always set to a value within [100.0, 1, 000.0].

Obviously, by training DualGAN, unlabeled and unpaired data can be converted from  $U$  to the corresponding data in  $V$  because the two data have some similar characteristics. Inspired by DualGAN, single channel blind source separation can be realized by converting the mixtures to the corresponding multiple sources which have similar characteristics. In this paper, we develop a PDualGAN to train multiple DualGAN simultaneously, the mixtures can be converted to corresponding multiple sources.

### III. MATHEMATICAL MODEL MODEL

The linear instantaneous mixed model and the convolutional mixed model are the most basic and important in single channel blind source separation.

#### 1) Linear instantaneous mixed model.

For linear instantaneous mixed model, the observed mixture  $X(t)$  can be defined as

$$X(t) = \sum_{i=1}^N A_i(t) s_i(t); \quad (4)$$

where  $X(t)$  is a observed mixture,  $s_i(t)$  is the  $i$ th source,  $A_i(t)$  is the  $i$ th mixing matrix.  $i = 1, 2, \dots, N$ .

#### 2) Convolutional mixed model.

For convolutional mixed model, the observed mixture  $X(t)$  can be defined as

$$X(t) = \sum_{i=1}^N A_i(t) * s_i(t); \quad (5)$$

where  $X(t)$  is a observed mixture,  $s_i(t)$  is the  $i$ th source,  $A_i(t)$  is the  $i$ th mixing matrix.  $i = 1, 2, \dots, N$ ,  $*$  denotes a convolution operation which can be defined as

$$A_i(t) * s_i(t) = \sum_{v=1}^N A_i(t-v) s_i(v); \quad (6)$$

where  $t$  is the amount of displacement of  $A(-v)$ . So (5) can be described as

$$X(t) = \sum_{i=1}^N A_i(t-v) s_i(v); \quad (7)$$

We can see from (4) and (7) that both the linear instantaneous mixed model and the convolutional mixed model can be regarded as a form of matrix multiplication, and a mixed signal corresponds to multiple sources. The aim of this paper is to find the one-to-multiple mapping relationship between the mixtures and the corresponding multiple sources.

### IV. PDUALGAN ALGORITHM

In this section, we present a PDualGAN algorithm to address the problem of separating multiple sources based on (4) and (7) which is applied to one-dimensional and two-dimensional signals. As shown in Fig. 3, we transform the problem of SCBSS into a data conversion problem in different domains with PDualGAN which is applied to train  $N$  DualGAN simultaneously. The first step is to train the PDualGAN with the mixtures which are mixed in random proportions and the corresponding sources, and save the results. The second step is to test the effect with different mixed proportions.

In our algorithm, no specific domain knowledge or pre-trained domain representation is needed, but the mapping relationship between unpaired signals is searched. The reconstruction error measures the disparity between the original signals and the reconstructed signals.  $N$  DualGANs are included in PDualGAN, each DualGAN has the same structure as shown in Fig. 4. The mixed signals are sampled from  $U$  and the corresponding sources are sampled from  $V_1, V_2, \dots, V_N$  respectively. The primary task of our PDualGAN is to build

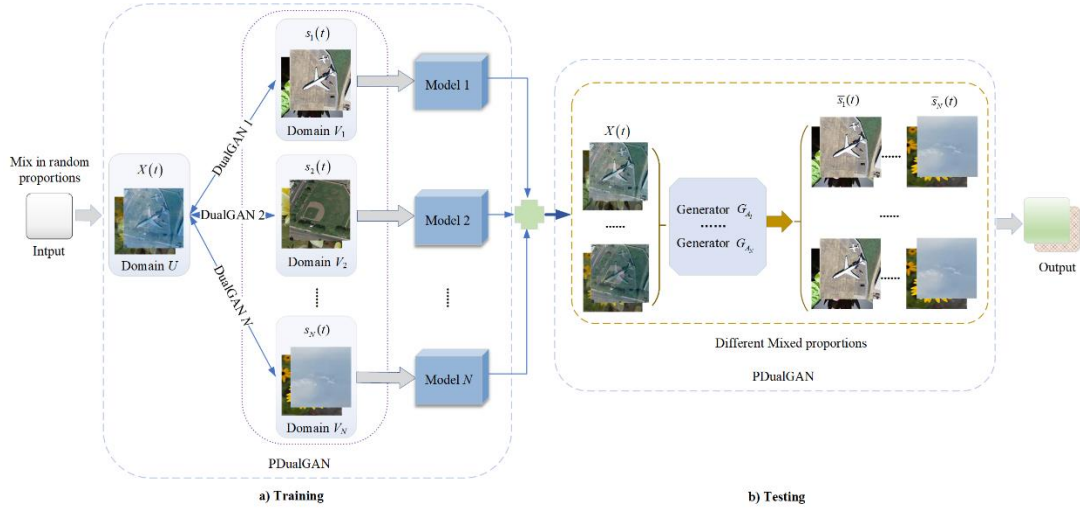


Fig. 3. The architecture of PDualGAN algorithm, including the training of PDualGAN a), N DualGAN are trained simultaneously, which learns the mapping between the mixture  $X(t)$  and the corresponding sources sequentially, each DualGAN learns one of these mappings. The testing of PDualGAN b), including several mixtures of different mixed proportions (different from the mixing proportions of training), the mixture  $X(t)$  as the input, and N estimated sources  $\hat{s}_1(t), \hat{s}_2(t), \dots, \hat{s}_N(t)$  as the Output.

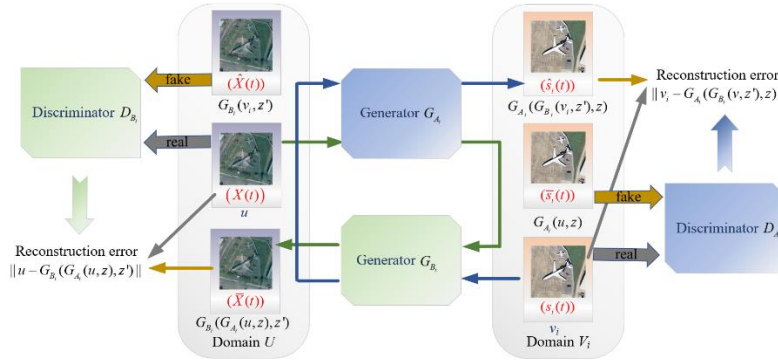


Fig. 4. Working process of each DualGAN.

the one-to-multiple mapping from  $X(t) \in U$  to  $s_1(t), s_2(t), \dots, s_N(t) \in V_1, V_2, \dots, V_N$ .

**Network configuration.** Each DualGAN in our PDualGAN has identical network architecture for  $G_{Ai}$  and  $G_{Bi}$ . The generator has the equal number of upsampling and downsampling layers, and skip connections are configured between them which became a U-shaped net [29] [30], such a structure enables low-level information to be shared signal input and output. In addition,  $z$  and  $z'$  are available only in the form of dropout and applied to multiple layers of generators at both training and testing phases, but they are not explicitly provided. For discriminators, the Markovian PatchGAN architecture is applied as described in [31], which is effective in capturing local high-frequency features (such as texture and style), and its effectiveness has been verified on various conversion tasks [27]. Furthermore, it requires fewer parameters, runs fast. Such a scheme fulfills our needs for signal separation.

The number of critic iterations per generator iteration can be set to 2-4,  $\lambda_U$  and  $\lambda_{V_i}$  are all set to 1000, an initial learning rate is set to 0.00005, and the batch size is assigned with 1.

The clipping parameter is set in [0.01, 0.1], and the epoch is set to 20000.

**Training.** Due to the momentum-based methods (such as adam) would occasionally lead to instability, we use mini-batch Stochastic Gradient Descent and apply the RMSProp solver which is known to perform well on highly nonstationary problems [28]. The sigmoid cross-entropy loss of traditional GAN is locally saturated and may cause the gradient to disappear. However, Wasserstein GAN gradient penalty (WGAN-GP) loss is differentiable almost everywhere, resulting in a better discriminator which can provide more reliable gradient information.

As shown in Fig. 3 a) and Fig. 4, for a mixture, a generator  $G_{Ai}$ :  $U \rightarrow V_i$  in the DualGAN  $i$  is learned by mapping the mixture  $u$  to a generated corresponding source  $G_{Ai}(u, z)$ , while the dual task is to train an inverse generator  $G_{Bi}$ :  $V_i \rightarrow U$  that maps a generated source  $G_{Ai}(u, z)$  to a generated mixture  $G_{Bi}(G_{Ai}(u, z), z')$ , where  $z$  and  $z'$  are random noises. N corresponding sources are simultaneously generated from a same mixture by N DualGAN (i.e.  $i=1, 2, \dots, N$ ) with the



identical structure.

For an original source, a generator  $G_{B_i}: V_i \rightarrow U$  in the DualGAN  $i$  is learned by mapping the source  $v_i$  to a generated mixture  $G_{B_i}(v_i, z')$ , while the dual task is to train an inverse generator  $G_{A_i}: U \rightarrow V_i$  that maps a generated mixture  $G_{B_i}(v_i, z')$  to a generated source  $G_{A_i}(G_{B_i}(v_i, z'), z)$ , where  $z$  and  $z'$  are random noises.  $N$  different sources generate the same mixture by  $N$  DualGAN (i.e.  $i=1,2,\dots, N$ ) with the identical structure.

The discriminator  $D_{A_i}$  discriminates the real source  $v_i$  of domain  $V_i$  and the fake outputs  $G_{A_i}(u, z)$ . The discriminator  $D_{B_i}$  discriminates the real mixture  $u$  of domain  $U$  and the fake outputs  $G_{B_i}(v_i, z')$ .

The same loss function is applied in each DualGAN for generators  $G_{A_i}$  and  $G_{B_i}$  which is defined as

$$\begin{aligned} I^{G_i}(u; v_i) = & \lambda_U \|u - G_{B_i}(G_{A_i}(u; z); z')\| \\ & + \lambda_{V_i} \|v_i - G_{A_i}(G_{B_i}(v_i; z'); z)\| \\ & - D_{B_i}(G_{B_i}(v_i; z')) - D_{A_i}(G_{A_i}(u; z)); \end{aligned} \quad (8)$$

where  $u \in U$ ,  $v_i \in V_i$ , and  $\lambda_U, \lambda_{V_i}$  are two constant parameters which are set to a value within  $[100.0, 1, 000.0]$ .

The corresponding loss functions applied in  $D_{A_i}$  and  $D_{B_i}$  are defined as:

$$I_{A_i}^D(u; v_i) = D_{A_i}(G_{A_i}(u; z)) - D_{A_i}(v_i); \quad (9)$$

$$I_{B_i}^D(u; v_i) = D_{B_i}(G_{B_i}(v_i; z')) - D_{B_i}(u); \quad (10)$$

where  $u \in U$ ,  $v_i \in V_i$ .

The one-to-multiple mapping between a mixture  $u \in U$  and  $N$  sources  $v_1, v_2, \dots, v_N \in V_1, V_2, \dots, V_N$  respectively which is built by training the proposed PDualGAN.

Testing. As shown in Fig. 3 b), with training the proposed PDualGAN, we save the trained model and parameters as the inputs of the test. The mixtures of different mixed proportions can be converted to corresponding multiple sources, which achieve the purpose of separating multiple sources from a mixture.

---

#### Algorithm 1 PDualGAN Algorithm

---

Input: The mixture  $u \in U$ , original sources  $v_i \in V_i$ ,  $i = 1, 2, \dots, N$ ,  $\lambda_U, \lambda_{V_i}$ , initial learning rate, batch size, clipping parameter.

Output: One-to-multiple corresponding estimated sources of  $u \in U$  to  $v_i \in V_i$ ,  $i = 1, 2, \dots, N$ .

- 1: Each mixture  $X(t)$  is mapping to  $N$  corresponding source  $s_1(t), s_2(t), \dots, s_N(t)$  by  $N$  generators  $G_{A_1}, G_{A_2}, \dots, G_{A_N}$ , and  $N$  original sources are mapping to the same mixture by  $N$  generators  $G_{B_1}, G_{B_2}, \dots, G_{B_N}$  simultaneously, and save the parallel results.  
Calculate loss function of generators  $G_{A_i}$  and  $G_{B_i}$  in each DualGAN.  
Calculate loss function of discriminators  $D_{A_i}$  and  $D_{B_i}$  in each DualGAN.
  - 2: end for.
  - 3: until convergence.
- 

## V. NUMERICAL EXPERIMENTS

In this section, the experiment is conducted to demonstrate the performance of the proposed PDualGAN algorithm, both one-dimensional and two-dimensional signals are used in the experiment.

Experimental data. Taking four sources as an example, we use four kinds of datasets for the experiment: the NWPU-occlusion image datasets, the ancient Chinese character occlusion datasets, the speech datasets, and the EEG datasets.

Each dataset including two types: (1) linear mixed signals and corresponding sources; (2) convolutional mixed signals and corresponding sources.

[NWPU-occlusion image datasets] A NWPU-occlusion image dataset including the original images selected from the NWPU-RESISC dataset<sup>1</sup> containing 45 categories and cloud and fog occlusion images captured by us. Each mixed image is mixed in random proportions by two NWPU-RESISC images and two cloud and fog occlusion images.

[Ancient Chinese character occlusion datasets] An ancient Chinese character occlusion dataset including the ancient Chinese character images and occlusion images we build. Each mixed image is mixed in random proportions by one ancient Chinese character image and three occlusion images.

[Speech datasets] The speech signals are selected from the THCHS-30 dataset<sup>2</sup> and randomly clipped 16384 points in each recorded sentence and normalized. Each mixed signal is mixed in random proportions by four original speech signals we selected.

THCHS-30 dataset was recorded by a single carbon microphone in a quiet office environment, with a total duration of more than 30 hours. Most of the speakers are college students who can speak fluent Mandarin. The sampling frequency is 16 kHz, and the sampling size is 16 bits. A total of 1000 recordings are involved.

[EEG datasets] The EEG acquisition equipment used in the experiment is the EEG and evoked potential meter (model NCERP-T-240) of Shanghai Nuocheng Electric Co., Ltd. we use 24-channel silver-plated electrodes, and the electrode placement position adopts the international standard 10/20. And the attention device developed by us to test the attention of the participants, which is developed based on the TGAM chip, and the attention threshold  $p$  can be set. When the attention of the participant is detected to be higher than the pre-defined threshold  $p$  (such as  $p > 60$ ), it indicates that the participant is focused on auditory stimulation. At this time, EEG signals can be collected.

A total of 50 participants are included in the EEG signal collection, of which 25 are males and 25 are females, aged between 20-40. All participants are either teachers or students from Taiyuan University of Science and Technology who are in good health and meet the requirements for EEG collection experiments.

We select the EEG signals according to the positions of the EEG electrodes of the temporal and frontal lobes and pre-processing them to remove artifacts such as ECG and oculus, then we randomly clipped 16384 points in each channel and normalize and convert the selected EEG signals into a multi-dimensional matrix to construct an EEG dataset. Each mixed signal is mixed in a random proportion by four original EEG signals we built.

Our PDualGAN algorithm is compared with the state-of-the-art algorithms on these four kinds of signals. The four kinds of datasets are used to train our network, all the datasets are pre-processed, each mixture corresponds to four sources

<sup>1</sup><https://hyper.ai/datasets/5449>

<sup>2</sup><http://www.openslr.org/resources/18/data>

that are mixed in random proportions, which as the input data of the PDualGAN network. Finally, several mixtures of different proportions are selected as test signals to demonstrate the effectiveness of the proposed algorithm.

**Baseline method** We compare our PDualGAN algorithm with linear mixed algorithms and convolutional mixed algorithms. Linear mixed algorithms including EMD-ICA (empirical mode decomposition and independent component analysis) [15], EEMD-PCA-ICA (ensemble empirical mode decomposition and principal component analysis and independent component analysis) [16], CEEDMAN-ICA (complete ensemble empirical mode decomposition with adaptive noise and independent component analysis) [32] and SSA-ICA (singular spectrum analysis and independent component analysis) [33] algorithms. Convolutional mixed algorithms including Conjugate Gradient [36], IRLS [36], S-D (synthesis-decomposition) [21], and DCSS (Single-channel blind deconvolution algorithm based on deep convolution generating adversarial network) [22] algorithms.

The facilities applied to perform the experiments include Intel I9-10900X 13.7 GHz CPU, 2\*NVIDIA RTX 8000 Graphics Card and 6\*32 GB memory. EMD-ICA [15], EEMD-PCA-ICA [16], CEEDMAN-ICA [32], SSA-ICA [33] and Conjugate Gradient [36], IRLS [36] are implemented in MATLAB. TABLE I shows the results of our algorithm as compared with the state-of-the-art algorithms in mean values of PSNR and correlation on four different datasets. Obviously, the proposed PDualGAN algorithm has better performance than the linear mixed algorithms: EMD-ICA, EEMD-PCA-ICA, CEEDMAN-ICA, SSA-ICA, and convolutional mixed algorithms: Conjugate Gradient [36], IRLS [36], S-D [21], DCSS [22] algorithms.

TABLE I  
THE PERFORMANCE OF OUR ALGORITHM AS COMPARED WITH  
STATE-OF-THE-ART ALGORITHMS ON FOUR DIFFERENT DATASETS.

Linear mixed Algorithm	PSNR	Correlation
EMD-ICA	7.52	0.2403
EEMD-PCA-ICA	7.90	0.2496
CEEDMAN-ICA	7.35	0.2076
SSA-ICA	8.70	0.2842
PDualGAN	24:63	0:7945
Convolutional mixed Algorithm	PSNR	Correlation
Conjugate Gradient	4.62	0.1942
IRLS	4.23	0.1570
S-D	11.29	0.5249
DCSS	11.85	0.5576
PDualGAN	22:97	0:7542

For the experiments on the NWPU-occlusion image datasets and ancient Chinese character occlusion datasets, the performance of the proposed PDualGAN algorithm can be evaluated by the peak signal-to-noise ratio (PSNR) [34] and correlation [35]. For the experiments on the speech datasets and EEG datasets, the performance of the proposed PDualGAN algorithm can be evaluated by correlation [35].

A higher PSNR value and correlation means a better effect of separating multiple sources, and a more closer the estimated source to the real source.

#### A. PDualGAN for NWPU-occlusion images.

In the first set of simulations, we evaluate the separating performance of the proposed PDualGAN algorithm described in Algorithm 1 on the NWPU-occlusion image datasets.

In the testing, we randomly select three groups of numbers from the NWPU-occlusion datasets. In Fig. 5, we show the test results of separating four images from linear mixtures, of which the mixtures are mixed in different random proportions. Fig. 6 shows the comparison results of average PSNR values obtained by the proposed PDualGAN algorithm and EMD-ICA, EEMD-PCA-ICA, CEEDMAN-ICA, SSA-ICA algorithms. Table II shows the comparison results of average correlation obtained by the proposed PDualGAN algorithm and the four state-of-the-art algorithms.

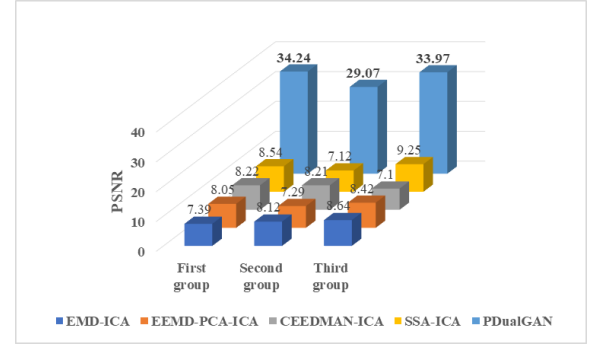


Fig. 6. Average PSNR of the proposed PDualGAN as compared with four state-of-the-art linear mixed algorithms.

TABLE II  
AVERAGE CORRELATION OF THE PROPOSED PDUALGAN AS COMPARED  
WITH FOUR STATE-OF-THE-ART LINEAR MIXED ALGORITHMS IN  
DIFFERENT PROPORTIONS.

Algorithm	First group	Second group	Third group
EMD-ICA	0.2077	0.2132	0.2692
EEMD-PCA-ICA	0.2780	0.1401	0.3101
CEEDMAN-ICA	0.1494	0.2136	0.1917
SSA-ICA	0.3451	0.1437	0.2117
PDualGAN	0:9531	0:9326	0:9640

As observed from Fig. 6 and TABLE II, the average PSNR of the proposed algorithm can reach 34.24 dB, the average correlation can reach 0.9640, which are higher than the EMD-ICA, EEMD-PCA-ICA, CEEDMAN-ICA and SSA-ICA algorithms. Therefore, the PDualGAN algorithm achieves better results than the baseline linear mixed algorithms in terms of both PSNR and correlation.

#### B. PDualGAN for ancient Chinese character occlusion images.

In the second set of simulations, we evaluate the separating performance of the proposed PDualGAN algorithm described in Algorithm 1 on the ancient Chinese character occlusion image datasets.

The testing is similar to section A. Fig. 7 shows the test results of separating four images from convolutional mixtures,

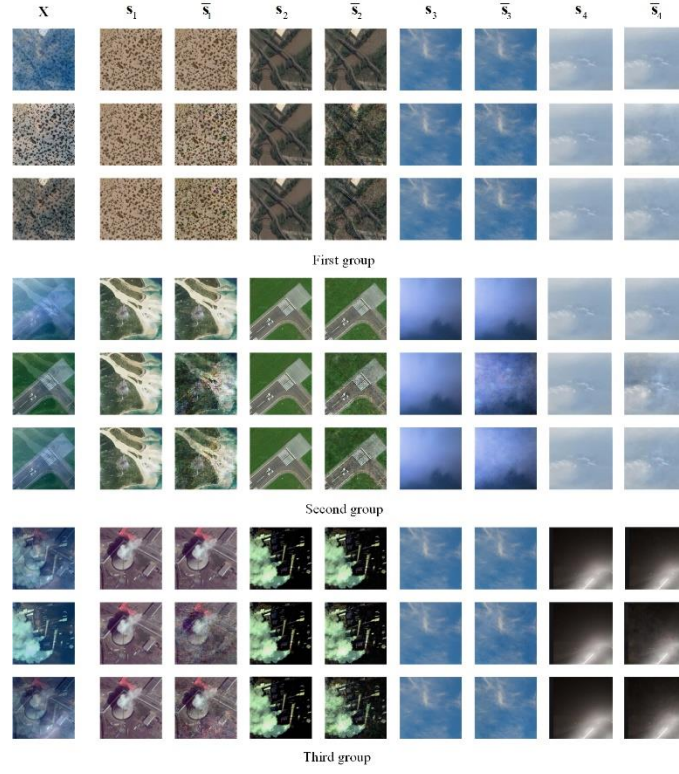


Fig. 5. Testing results of PDualGAN approach for linear mixed images. Each group including three mixtures mixed in different random proportions of four same images. (different from the mixing proportions of training). The  $X$  represents the mixture,  $s_1$ ,  $s_2$ ,  $s_3$ , and  $s_4$  represent the four original ground-truth sources,  $\bar{s}_1, \bar{s}_2, \bar{s}_3, \bar{s}_4$  represent the corresponding estimated sources.

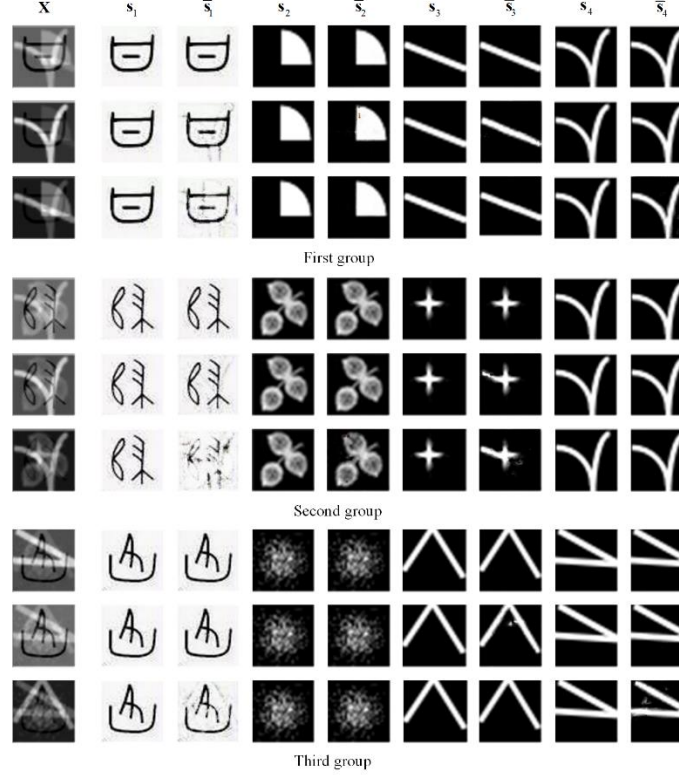


Fig. 7. Testing results of PDualGAN approach for convolutional mixed images. Each group including three mixtures mixed in different random proportions of four same images. The  $X$  represents the mixture,  $s_1$ ,  $s_2$ ,  $s_3$ , and  $s_4$  represent the four original ground-truth sources,  $\bar{s}_1, \bar{s}_2, \bar{s}_3, \bar{s}_4$  represent the corresponding estimated sources.



of which the mixtures are mixed in different random proportions. We compared the PDualGAN algorithm with Conjugate Gradient, IRLS, S-D and DCSS algorithms according to the different mixed proportions of Fig. 7. The comparison results of average PSNR values and average correlation obtained by different algorithms are shown in Fig. 8 and TABLE III respectively. Obviously, the average PSNR of the PDualGAN algorithm can reach 38.98 dB, and the average correlation can reach 0.9933, which is far more better than the four baseline algorithms.

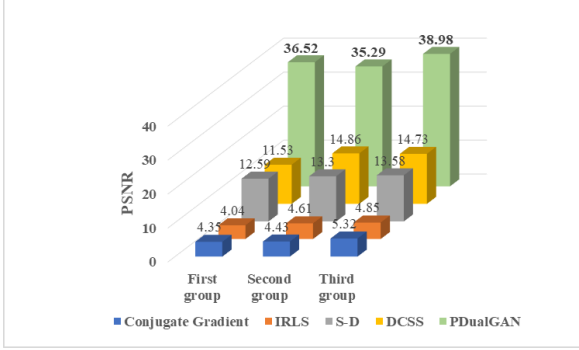


Fig. 8. Average PSNR of the proposed PDualGAN as compared with four state-of-the-art convolutional mixed algorithms.

TABLE III

AVERAGE CORRELATION OF THE PROPOSED PDUALGAN AS COMPARED WITH FOUR STATE-OF-THE-ART CONVOLUTIONAL MIXED ALGORITHMS IN DIFFERENT PROPORTIONS.

Algorithm	First group	Second group	Third group
Conjugate Gradient	0.2395	0.1491	0.3152
IRLS	0.1513	0.0921	0.2372
S-D	0.5864	0.5004	0.6720
DCSS	0.5077	0.6485	0.6081
PDualGAN	0:9863	0:9432	0:9933

### C. PDualGAN for speech signals.

In the third set of simulations, we evaluate the separating performance of the proposed PDualGAN algorithm described in Algorithm 1 on the speech signal datasets.

The testing is similar to section A. We randomly select three groups of numbers from the speech dataset. Fig. 9 shows the test results for convolutional mixed signals with two mixtures mixed in different random proportions. Similarly, we compared the PDualGAN algorithm with Conjugate Gradient, IRLS, S-D and DCSS algorithms according to the different mixed proportions shown in Fig. 9. TABLE IV demonstrates the comparison results of the correlation obtained by the four different algorithms.

As shown in TABLE IV, the proposed PDualGAN algorithm can obtain an average correlation of 0.9656, which is better than the Conjugate Gradient, IRLS, S-D and DCSS algorithms.

### D. PDualGAN for EEG signals.

In the fourth set of simulations, we evaluate the separating performance of the proposed PDualGAN algorithm described in Algorithm 1 on the EEG signal datasets.

TABLE IV

AVERAGE CORRELATION OF THE PROPOSED PDUALGAN AS COMPARED WITH FOUR STATE-OF-THE-ART CONVOLUTIONAL MIXED ALGORITHMS IN DIFFERENT PROPORTIONS.

Algorithm	First group	Second group	Third group
Conjugate Gradient	0.4267	0.0907	0.1842
IRLS	0.1559	-0.0112	0.0091
S-D	0.6207	0.6582	0.5879
DCSS	0.5643	0.6496	0.6839
PDualGAN	0:9656	0:7012	0:7280

The testing is similar to section A. Fig. 10 shows the test results for convolutional mixed signals with two mixtures mixed in different random proportions. Similarly, we compared the PDualGAN algorithm with EMD-ICA, EEMD-PCA-ICA, CEEDMAN-ICA, SSA-ICA algorithms according to the different mixed proportions shown in Fig. 10. TABLE V demonstrates the comparison results of the correlation obtained by different algorithms.

TABLE V

AVERAGE CORRELATION OF THE PROPOSED PDUALGAN AS COMPARED WITH FOUR STATE-OF-THE-ART LINEAR ALGORITHMS IN DIFFERENT PROPORTIONS.

Algorithm	First group	Second group	Third group
EMD-ICA	0.0181	0.0071	0.0043
EEMD-PCA-ICA	0.0253	0.0325	0.0297
CEEDMAN-ICA	0.0906	0.0348	0.0537
SSA-ICA	0.0130	0.0057	0.0186
PDualGAN	0:7227	0:9743	0:7162

The experimental results show that the proposed PDualGAN algorithm outperforms state-of-the-art algorithms in both P-SNR and correlation on the four different datasets for the linear instantaneous mixed model and the convolutional mixed model, which shows the effectiveness of this method.

## VI. CONCLUSION

In this paper, a new algorithm for the problem of single channel blind source separation (SCBSS) has been presented. Our contributions are as follows:

Model. We have found the relevant expression to describe the common characteristics of the linear instantaneous mixed model and convolutional mixed model for the research.

Algorithm. Based on the linear instantaneous mixing model and convolutional mixed model, we proposed a PDualGAN algorithm. N DualGAN are trained simultaneously with mixtures and corresponding sources to realize one-to-multiple mapping, and Wasserstein generative adversarial networks gradient penalty(WGAN-GP) loss function is applied to improve the stability of the network.

The proposed algorithm can be applied to both one-dimensional and two-dimensional signals, and different mixed proportions are used to test the effectiveness and generalization performance.

Datasets. We build the one-to-multiple datasets in the experiment which are composed of two parts: the mixtures and corresponding sources. Each mixture is mixed in a random proportion by multiple corresponding sources which are



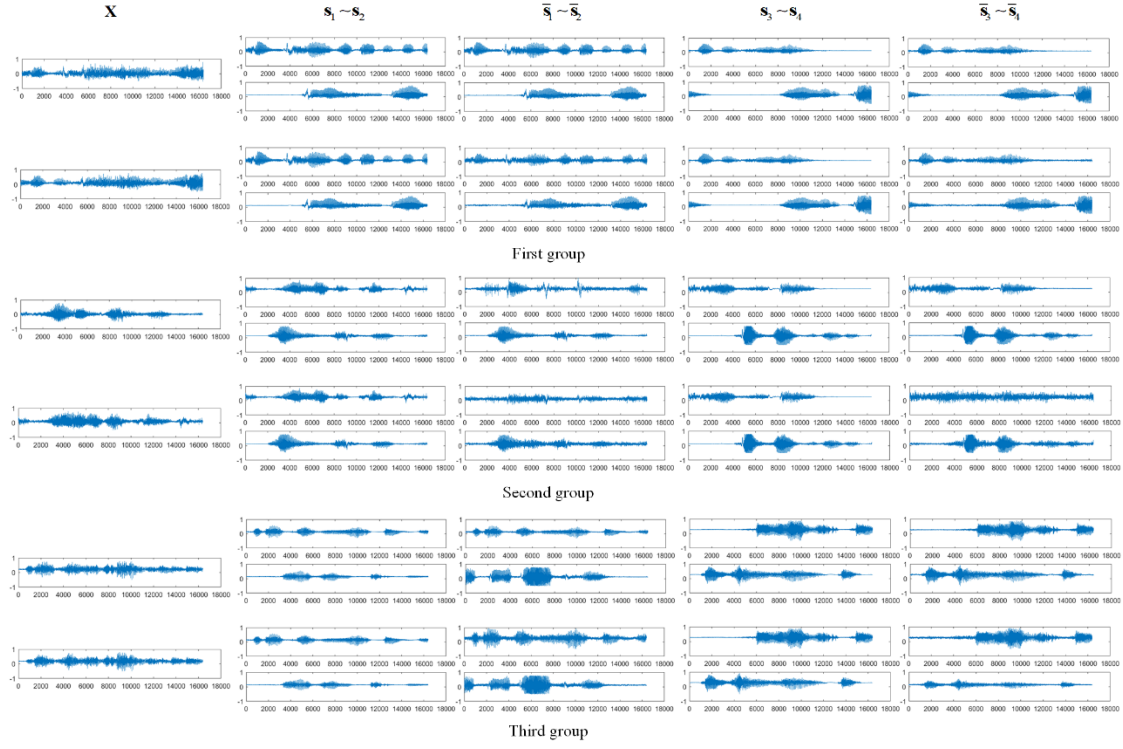


Fig. 9. Testing results of PDualGAN approach for convolutional mixed signals. Each group including two mixtures mixed in different random proportions of four same signals. The  $X$  represents the mixture,  $s_1$ ,  $s_2$ ,  $s_3$ , and  $s_4$  represent the four original ground-truth sources,  $\hat{s}_1, \hat{s}_2, \hat{s}_3, \hat{s}_4$  represent the corresponding estimated sources.

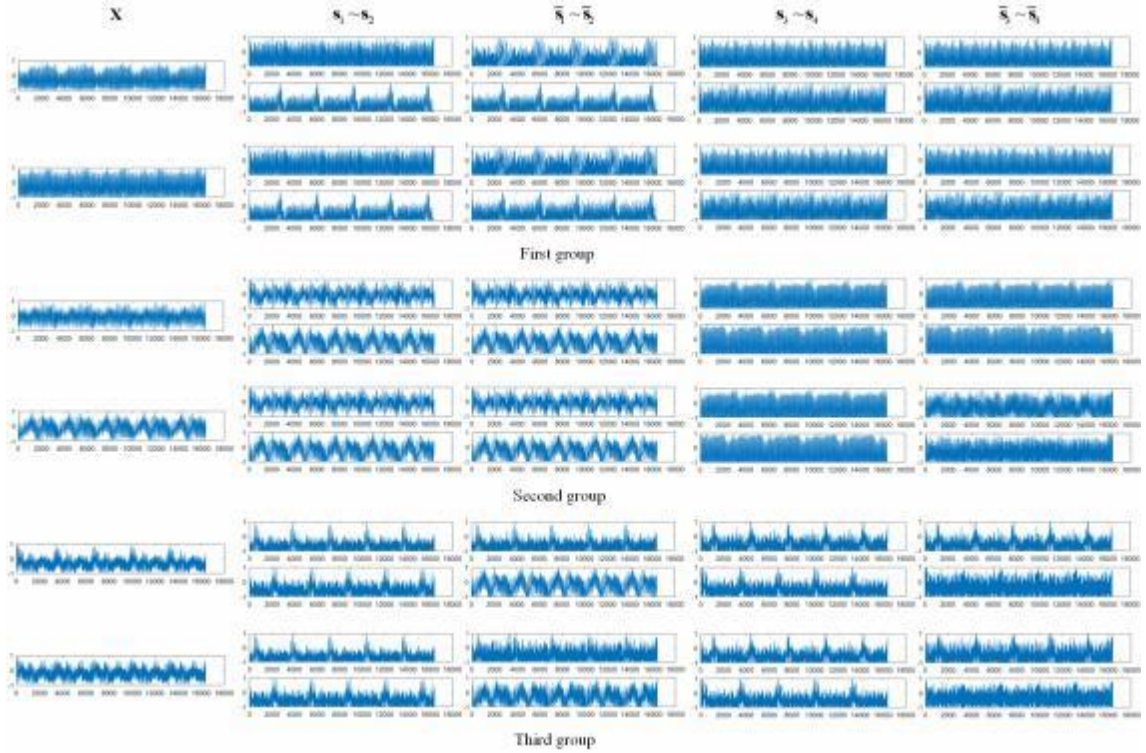


Fig. 10. Testing results of PDualGAN approach for linear mixed signals. Each group including two mixtures mixed in different random proportions of four same signals. The  $X$  represents the mixture,  $s_1$ ,  $s_2$ ,  $s_3$ , and  $s_4$  represent the four original ground-truth sources,  $\hat{s}_1, \hat{s}_2, \hat{s}_3, \hat{s}_4$  represent the corresponding estimated sources.

randomly selected. These datasets can be used for related research.

Numerical experiments show that the proposed PDualGAN algorithm performs well in separating multiple sources from linear mixed signals or convolutional mixed signals which outperforms the EMD-ICA, EEMD-PCA-ICA, CEEDMAN-ICA, SSA-ICA, Conjugate Gradient, IRLS, S-D and DCSS algorithms.

#### ACKNOWLEDGMENT

This study was supported by the China Scholarship Council under Grant [2020]1417, the Key Research and Development Project of Shanxi Province under Grant 201803D421035, the Natural Science Foundation for Young Scientists of Shanxi Province under Grant 201901D211313, the Research, Teaching, and Research Funding Project of Shanxi Province for Returned Overseas Students under Grant HGKY2019080. The authors would like to thank the anonymous reviewers for their constructive comments improving this article.

#### REFERENCES

- [1] P. K. Krishna, K. Ramaswamy. Single channel speech separation based on empirical mode decomposition and hilbert transform. *IET Signal Proc.*, vol. 11, no. 5, pp. 579-586, 2017.
- [2] F. Fan, K. Yang, M. Xia, et al. Underwater image restoration by means of blind deconvolution approach. *Front. Optoelectron. China*, vol. 3, no. 2, pp. 169-178, 2010.
- [3] C. J. James, S. Wang. Blind source separation in single-channel EEG analysis: an application to BCI. *Annu Int Conf IEEE Eng Med Biol Proc*, pp: 6544-6547, 2006.
- [4] Y. Zheng, Z. Jiang, H. Zhang, et al. Size-scalable content-based histopathological image retrieval from database that consists of WSIs. *IEEE J. Biomedical Health Informat.*, vol. 22, no. 4, pp. 1278-1287, 2018.
- [5] W. P. Segars, B. M. W. Tsui, J. Cai, et al. Application of the 4-D XCAT phantoms in biomedical imaging and beyond. *IEEE Trans. Med. Imaging.*, vol. 37, no. 3, pp. 680-692, 2018.
- [6] D. V. Sorokin, I. Peterlik, M. Tektonidis, et al. Non-rigid contour-based registration of cell nuclei in 2-D live cell microscopy images using a dynamic elasticity model. *IEEE Trans. Med. Imaging.*, vol. 37, no. 1, pp. 173-184, 2018.
- [7] Y. Guo, A. Wang, W. Wang. Multi-source phase retrieval from multi-channel phaseless STFT measurements. *Signal Process*, vol. 144, pp. 36-40, 2018.
- [8] Y. Guo, T. Wang, J. Li, et al. Multiple Input Single Output Phase Retrieval. *Circ Syst Signal Process*, vol. 38, no. 8, pp. 3818-3840, 2019.
- [9] Y. Guo, X. Zhao, J. Li, et al. Blind Multiple Input Multiple Output Image Phase Retrieval. *IEEE Trans Ind Electron*, vol. 67, no. 3, pp. 2220-2230, 2020.
- [10] B. Gao, L. Bai, W. L. Woo, et al. Automatic Defect Identification of Eddy Current Pulsed Thermography Using Single Channel Blind Source Separation. *IEEE Trans. Instrum. Meas.*, vol. 63, no. 4, pp. 913-922, 2014.
- [11] C. C. Wang, Y. H. Zeng. Research Status and Prospects of Underdetermined Blind Source Separation Algorithms. *J Beijing Univ Posts and Telecommun.* vol. 41, no. 6, pp. 103-109, 2018.
- [12] L. S. Zhan, D. S. Huang, C. H. Zheng, et al. Blind inversion of Wiener system for single source using nonlinear blind source separation, *Proc Int Jt Conf Neural Networks*, vol. 2, pp. 1235-1238, 2005.
- [13] L. D. Persia, Diego H. Milone, M. Yanagi. Pseudoanechoic blind source separation with improved Wiener postfilter. 2009.
- [14] Z. Zhao, X. Yan. Algorithm for EMD and ICA-based Single-channel Voice Blind Source Separation. *Electron Sci Technol*, 2012.
- [15] B. Mijovic, M. Vos, I. Gligorijevic, et al. Source Separation From Single-Channel Recordings by Combining Empirical-Mode Decomposition and Independent Component Analysis. *IEEE Trans. Biomed. Eng.*, vol. 57, no. 9, pp. 2188-2196, 2010.
- [16] Y. Guo, S. Huang, Y. Li. Single-Mixture Source Separation Using Dimensionality Reduction of Ensemble Empirical Mode Decomposition and Independent Component Analysis. *Circ Syst Signal Process*, vol. 31, no. 6, pp. 2047-2060, 2012.
- [17] Y. Guo, S. Huang, Y. Li, et al. Edge Effect Elimination in Single-Mixture Blind Source Separation. *Circ Syst Signal Process*, vol. 32, no. 5, pp. 2317-2334, 2013.
- [18] D. D. LEE, H. S. SEUNG. Learning the Parts of Objects by Non-Negative Matrix Factorization. *Nature*, vol. 401, no. 6755, pp. 788-791, 1999.
- [19] B. Gao, W. L. Woo, S. S. Dlay. Single-Channel Source Separation Using EMD-Subband Variable Regularized Sparse Features. *IEEE Trans. Audio Speech Lang. Process.*, vol. 19, no. 4, pp. 961-976, 2011.
- [20] Y. C. Subakan, P. Smaragdis. Generative adversarial source separation. *ICASSP IEEE Int Conf Acoust Speech Signal Process Proc*, pp. 26-30, 2018.
- [21] Q. Q. Kong, Y. Xu, W. W. Wang, et al. Single-channel signal separation and deconvolution with generative adversarial networks. *IJCAI Int. Joint Conf. Artif. Intell.*, pp. 2747-2753, 2019.
- [22] T. Yin, T. Liu, Y. Guo. Research on Single-channel Blind Deconvolution Algorithm for Ancient Chinese Character Repair. *J. Chin. Comput. Sys.*, vol. 42, no. 2, pp. 414-417, 2021.
- [23] Z. Yi, H. Zhang, P. Tan, et al. DualGAN: Unsupervised Dual Learning for Image-to-Image Translation. In *Proc. IEEE Int. Conf. Comput Vision*, pp. 2868-2876, 2017.
- [24] I. Sucholutsky, M. Schonlau. Less Than One-Shot Learning: Learning N Classes From  $M < N$  Samples. *arXiv preprint arXiv: 2009.08449*, 2020.
- [25] J. C. Bezdek, L. I. Kuncheva. Nearest prototype classifier designs: An experimental study. *International Journal of Intelligent Systems*. vol. 16, no. 12, pp. 1445-1473, 2001.
- [26] I. Goodfellow, J. Pouget-Abadie, M. Mirza, et al. Generative adversarial nets. *Adv. neural inf. proces. syst.*, vol. 2, pp. 2672-2680, 2014.
- [27] Y. Xia, D. He, T. Qin, et al. Dual learning for machine translation. *Adv. neural inf. proces. syst.*, vol. 29, pp. 820-828, 2016.
- [28] M. Arjovsky, S. Chintala, and L. Bottou. Wasserstein gan. *arXiv preprint arXiv: 1701.07875*, 2017.
- [29] P. Isola, J. Y. Zhu, T. Zhou, et al. Image-to-image translation with conditional adversarial networks. *Proc. - IEEE Conf. Comput. Vis. Pattern Recognit, CVPR*, pp. 5967-5976, 2017.
- [30] O. Ronneberger, P. Fischer, and T. Brox. U-net: Convolutional networks for biomedical image segmentation. *Lect. Notes Comput. Sci.*, pp. 234-241, 2015.
- [31] M. Liu, T. Breuel, and J. Kautz. Unsupervised image-to-image translation networks. *Adv. neural inf. proces. syst.*, pp. 700-708, 2017.
- [32] Z. Luo, Z. Yan, F. U. Weidong, et al. Electroencephalogram Artifact Filtering Method of Single Channel EEG Based on CEEMDAN-ICA. *Chinese J. Sens. Actuators*, vol. 31, no. 8, pp. 1211-1216, 2018.
- [33] S. Jabbari. Source separation from single-channel abdominal phonocardiographic signals based on independent component analysis. *Biomed. Eng. Lett.*, vol. 11, no.1, pp. 55-67, 2021.
- [34] Q. Huynh-Thu and M. Ghanbari. Scope of validity of psnr in image/video quality assessment. *Electron. Lett.*, vol. 44, no. 13, pp. 800-801, 2008.
- [35] B. G. Hne, K. Jger, H. G. Drexler. The Pearson product-moment correlation coefficient is better suited for identification of DNA fingerprint profiles than band matching algorithms. *Electrophoresis*, vol. 14, no. 1, pp. 967-972, 1993.
- [36] A. Levin, R. Fergus, F. Durand, et al. Deconvolution using natural image priors. *ACM T Graphic*, vol. 6, pp. 0-2, 2007.